Effect of electron correlations on structural phase stability, magnetism, and spin-dependent transport in $CeMnNi_4$

M. S. Bahramy,[1,*] P. Murugan,[2] G. P. Das,[3] and Y. Kawazoe[1]
[1]*Institute for Materials Research, Tohoku University, Sendai 980-8577, Japan*
[2]*Central Electrochemical Research Institute, Karaikudi 630006, Tamil Nadu, India*
[3]*Indian Association for the Cultivation of Science, Jadavpur, Kolkata 700032, India*
(Received 2 March 2010; published 23 April 2010)

First-principles calculations are carried out to study the effect of electron correlations on relative structural stability, magnetism, and spin-dependent transport in $CeMnNi_4$ intermetallic compound. The correct description of Coulomb repulsion of Mn 3*d* electrons is shown to play a crucial role in reproducing the experimentally observed cubic phase of $CeMnNi_4$ as well as its relatively high degree of transport spin polarization (~66%). These are the two fundamental properties of this compound which conventional density-functional theory approaches fail to predict correctly. The reason for this failure is attributed to an extreme overdelocalization of Mn 3*d* charges causing a strong *d*-*d* hybridization between Mn and Ni atoms in the orthorhombic phase. Such an artificial hybridization, in turn, lowers the relative total energy of the orthorhombic phase with respect to the cubic one. It also leads to an incorrect carrier concentration and mobility at the Fermi level and, consequently, yields much lower degree of transport spin polarization for this nearly half-metallic compound.

DOI: 10.1103/PhysRevB.81.165114 PACS number(s): 72.25.−b, 31.15.V−, 61.66.Dk, 75.50.Cc

Electron correlation plays a crucial role in understanding the electronic structure and magnetism in narrow-band systems. Density-functional theory (DFT) within its local-density approximation (LDA) and generalized gradient approximation (GGA) turns out to be impressively successful in describing the ground-state properties of many materials. However, as an approximation, LDA/GGA faces serious difficulties for the strongly correlated systems, e.g. high-temperature oxide superconductors[1] and the middle-to-late transition-metal oxides.[2] Such a complication arises from the fact that the current implementations of DFT intrinsically tend to underestimate the Coulomb repulsion and, hence, fail to capture the correlation-driven charge localizations. Consequently, the conventional DFT calculations appear to underestimate or even close the band gap. They may even result in an incorrect description of the magnetic ground state.[3] Among the remedies to overcome this problem, the so-called LDA+*U* approach[3] has already proven to be computationally one of the most efficient methods to study a large variety of strongly correlated systems, with considerable improvements over LDA and GGA. In this method, a strong intra-atomic interaction is introduced in a screened Hartree-Fock-type manner as on-site replacement of the LDA (GGA). Since the introduction of LDA+*U* by Anisimov *et al.*,[3] this formalism has been extensively utilized to investigate the electronic and magnetic properties of narrow-band systems. However, it has rarely been used to predict the correct structural phase stability of strongly correlated systems.

It is already known that for some compounds, both LDA and GGA severely fail to predict the ground-state structure. An example for such systems is $CeMnNi_4$. It is a unique intermetallic soft ferromagnet (FM) discovered recently,[4] which exhibits large magnetic moment ($\sim 4.95 \mu_B$/Mn), reasonably high Curie temperature (~150 K), and a high degree of transport spin polarization *P* (~66%) as probed by point-contact Andreev reflection (PCAR) spectroscopy. Recent LDA and GGA calculations[5–7] for the cubic phase (CP) reveal the FM phase to be stable and the resulting magnetic moment as well as mean-field-estimated Curie temperature are in close agreement with the experimental data. What is, however, intriguing is that the DFT calculations have failed to reproduce (a) the correct ground-state structure which is cubic while the calculations indicate an orthorhombic phase (OP) (Ref. 7) and (b) the experimental *P* which is significantly higher than the calculated results.[6,8] In fact, the parent compound $CeNi_5$ which exhibits enhanced Pauli paramagnetism was also found to show some discrepancy between the experimental data and the LDA results.[9]

The reason for these discrepancies has been unclear so far. In this work, we explicitly show that within LDA+*U* formalism, with the correct choices for Coulomb *U* and exchange *J* on Mn 3*d* bands, not only the structural phase stability but also the spin-dependent transport is well reproduced for $CeMnNi_4$ as what has been observed experimentally.[4] Assuming that Ce 4*f* bands as well as Ni 3*d* bands may also be somewhat overdelocalized by LDA and GGA, we consider the effect of *U* correction on these bands and discover that such a correction hardly plays any role in addressing the above disagreements.

The electronic-structure calculations have been carried out using the gradient-corrected PW91 exchange-correlation functional[10,11] with inclusion of the on-site Coulomb *U* and the projected augmented wave method,[12] as implemented in the VASP code.[13] We have estimated for Mn 3*d* states the values of $U=7.0$ eV and $J=0.8$ eV from the first principles[3] using the linear muffin-tin orbital method.[14] Since the *U* parameter obtained from *ab initio* calculations appears to be larger than its actual value, we have considered the corresponding *U* value as an upper limit and instead have varied *U* on Mn 3*d* from 0 to 7.0 eV in order to arrive at its optimum value. We have independently varied *U* on Ce 4*f* and on Ni 3*d* within the same range as above, while the respective *J* values have been fixed to 0.33 eV (Ref. 6) and 0.95 eV.[3] We consider both the cubic and orthorhombic phases of

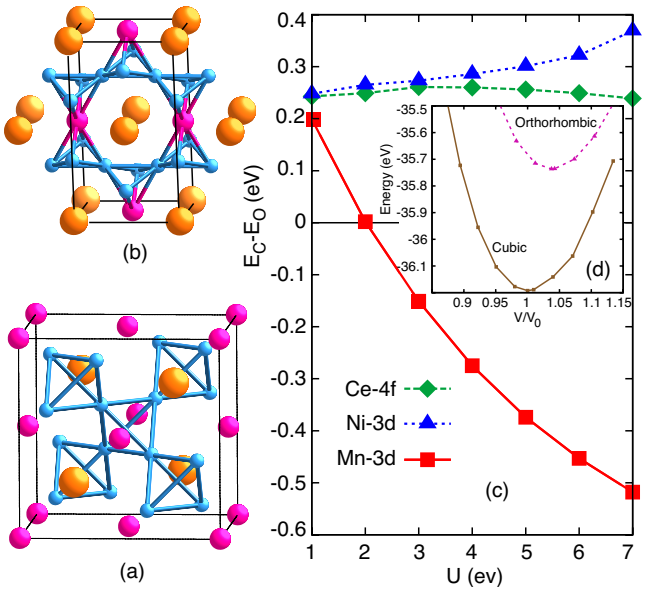

FIG. 1. (Color online) Crystal structure of (a) cubic and (b) orthorhombic $CeMnNi_4$. The large (orange), medium (purple), and small (blue) balls indicate Ce, Mn, and Ni, respectively. (c) The energy difference between cubic and orthorhombic phases as a function of U. (d) The relative structural stabilities of the cubic and orthorhombic phases of $CeMnNi_4$ as computed with $U=6.0$ eV and $J=0.8$ eV on Mn $3d$ bands.

$CeMnNi_4$. For the former (latter), a cubic (orthorhombic) supercell containing 4 (2) formula units of $CeMnNi_4$ is constructed and the corresponding Brillouin zone is sampled by a $20\times20\times20$ Monkhorst-Pack mesh. The structures have been fully optimized without any symmetry constraint, using the conjugate gradient method until the magnitude of force on each ion is less than 0.001 eV/Å. The degree of spin polarization P_n is computed with Mazin's equation[15] $P_n=\frac{\langle Nv_F^n\rangle_\uparrow-\langle Nv_F^n\rangle_\downarrow}{\langle Nv_F^n\rangle_\uparrow+\langle Nv_F^n\rangle_\downarrow}$ using the tetrahedron method.[8] Here, N is the density of states at Fermi energy, ε_F, and v_F is the Fermi velocity of electrons with spin σ ($\uparrow$ and $\downarrow$), respectively. The index n indicates the static (P_0), ballistic (P_1), and diffusive (P_2) limits.

Figures 1(a) and 1(b) show the respective crystal structures for CP and OP of $CeMnNi_4$. The former crystallizes in space group $F\bar{4}3m$. The previously calculated lattice constant $a=6.99$ Å using pure PW91 functional[7] slightly increases (decreases) by 1% by increasing U to 7.0 eV on Mn (Ni) $3d$ bands, while it remains insensitive to the variation in U on Ce $4f$. On the other hand, the orthorhombic structure belongs to the space group $P6/mmm$. The lattice constants $a=8.53$ Å, $b=4.93$ Å, and $c=4.06$ Å remain unchanged with variation in U on Ce and Ni, however, they tend to smoothly expand by ~2% by increasing U on Mn $3d$ to 7.0 eV. In contrast to CP, Mn is closely attached to the neighboring eight Ni atoms with distances ~2.47 Å.

We have calculated the energy difference between the FM-CP and FM-OP, $\Delta E=E_C-E_O$, as a function of U, where U on Ce $4f$, Mn $3d$, and Ni $3d$ have been varied independently. Figure 1(c) shows the respective results. The figure clearly indicates that varying U on Ce $4f$ has almost no effect on the structural stability. Throughout the whole range OP turns out to be energetically more stable than CP by ~0.25 eV. Applying U on Ni $3d$ bands, E_O still lies below E_C and even tend to decline very smoothly and almost linearly to relatively lower energy values as U increases. In contrast, by increasing U on Mn $3d$ states, one can notice that there is a strong tendency for CP to become energetically more stable as compared to OP. It is evident from Fig. 1(c), ΔE decreases so sharply with the increase in U on Mn that for $U>2.0$ eV the cubic structure of $CeMnNi_4$ becomes more stable. For the limiting value of $U_{\mathrm{Mn}}^{3d}=7.0$ eV, ΔE astonishingly goes below −0.5 eV, indicating the extent to which the ground-state structural stability would go wrong due to the under-representation of electron correlation effect. We anticipate the actual value of U_{Mn}^{3d} to be around 6.0 eV (the reason will be discussed later). For this value, we have plotted in Fig. 1(c) both E_C and E_O as a function of V/V_0, where V is the lattice volume and V_0 indicates the cubic lattice volume for which the total energy is minimum. The relative positions of energy minima for CP and OP reveal that in ground state the former always have a smaller lattice volume and there is no possible way for pressure-induced phase transition from cubic to orthorhombic structure.

To explain why variation in U on Mn $3d$ plays such a crucial role in defining the structural phase stability of $CeMnNi_4$, we have shown in Figs. 2 and 3, the respective partial density of states (PDOS) contributed from Ce $4f$, Mn $3d$, and Ni $3d$ states for CP and OP. For each structure, PDOS has been evaluated at various U (and J) values on Mn $3d$. At $U=0$, one can clearly see the Mn $3d$ states are substantially delocalized within a wide energy range. Such a delocalization is more enhanced in OP, where the spin-up Mn $3d$ states have a complete overlap with their corresponding Ni $3d$ counterparts. Additionally, in this phase the spin-down Mn $3d$ states turn out to be partially occupied (see Fig. 3), indicating that the exchange interaction among the two spin channels of Mn $3d$ states and, hence, the total magnetic moment (as will be discussed shortly) are relatively smaller in OP as compared to that in CP. Considering the fact that, in OP each Mn is surrounded by eight Ni with Mn-Ni distances much shorter than that in CP, it is logical to expect a much stronger d-d hybridization between Mn and Ni atoms in OP. This is the reason why OP is found to be energetically more stable than CP, within GGA (or even LDA).

Turning on U on Mn $3d$ states, one can notice a striking similarity between the PDOS of the two phases (see Figs. 2 and 3). For both, at $U=6.0$ eV the occupied Mn $3d$ states become substantially localized in a very narrow region far below ε_F. More importantly, there is almost no overlap between these states and the corresponding Ni $3d$ states, thereby resulting in a substantial reduction in hybridization between Mn $3d$ and Ni $3d$ states. As mentioned above, such a hybridization is expected to be considerably more effective in OP than in CP. In fact in the latter, the Mn atom appears to be separated from Ce and Ni atoms as it is somehow trapped in a large cavity with considerably large Mn-Ni and Mn-Ce distances ~2.89 Å and ~3.02 Å, respectively.[16] Moreover, the closed shape of Ni tetrahedra in CP [see Fig. 1(a)] implies that the d-d hybridization is dominant between the Ni atoms rather than between Ni and Mn atoms. On this basis,

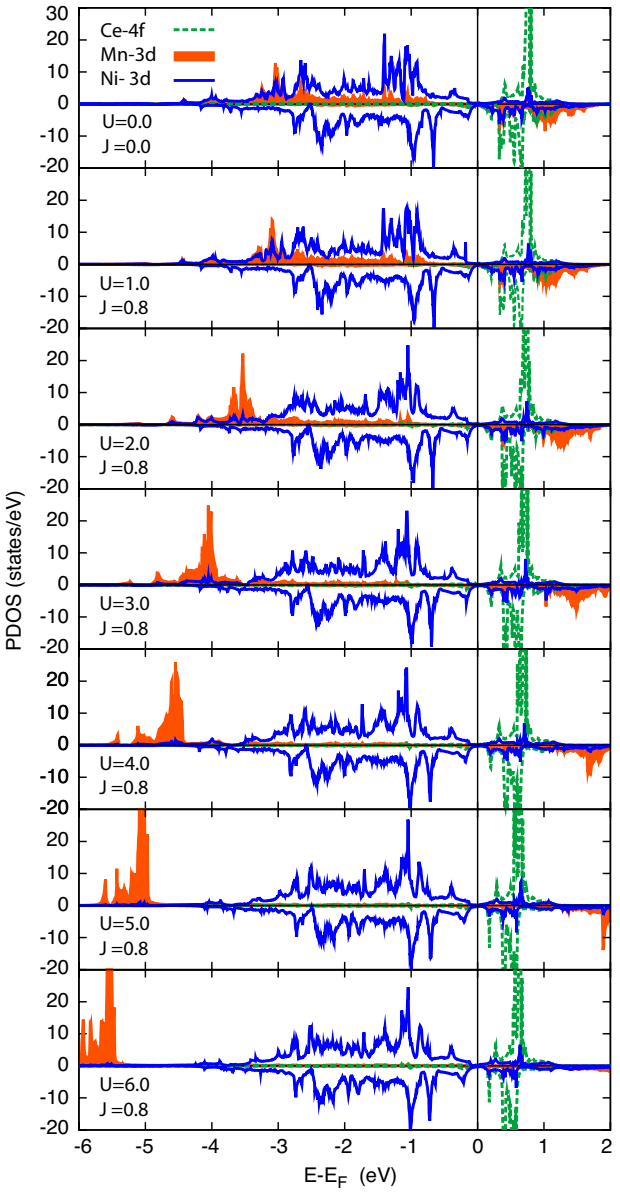

FIG. 2. (Color online) Partial density of states of the cubic phase of $CeMnNi_4$ as obtained for various U and J values (in eV).

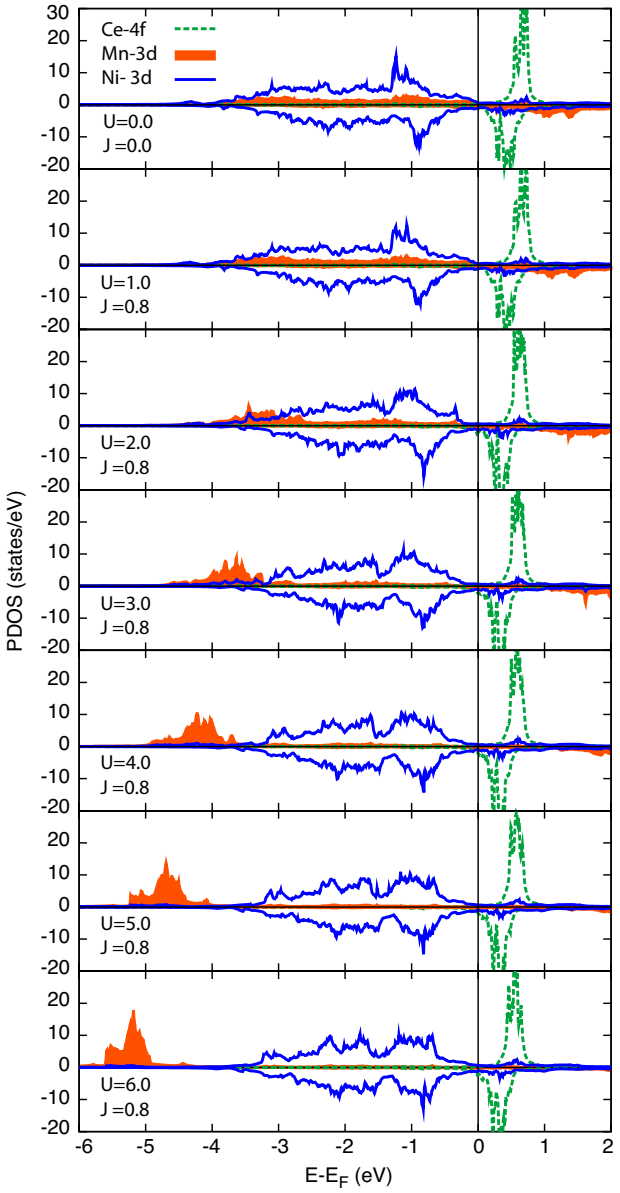

FIG. 3. (Color online) Partial density of states of the orthorhombic phase of $CeMnNi_4$ as obtained for various U and J values (in eV).

any reduction in Mn-Ni hybridization is expected to destabilize OP more effectively, thereby rendering the cubic structure to become energetically more stable. It is worth mentioning that from GGA calculations, the $4f$ bands of Ce turn out to be approximately 1 eV above ε_F (see Fig. 2). Varying U on these bands, we have only noticed a change in splitting of the two spin channels of $4f$ states, reasoning why ΔE is so much insensitive to the U variation on Ce $4f$.

As regards the magnetism, our LDA+U calculations reveal that for CP (OP) the FM configuration energetically lies below the antiferromagnetic and nonmagnetic configurations by 13 meV (11 meV) and 6.47 eV (4.07 eV), respectively. At U=0 and U=6.0 eV, the calculated total magnetic moments in the formula units are $4.85\mu_B$ ($3.70\mu_B$) and $5.00\mu_B$ ($4.45\mu_B$) for CP (OP), respectively. Evidently, the increase in U slightly increases the magnetic moment in CP while it significantly enhances the value of magnetic moment in OP. The reason, as described above, is due to the deficiency of GGA approach in treating the Mn $3d$ states, thereby leading to an artificial d-d hybridization between Mn and Ni atoms, which turns out to be much stronger in OP than in CP. Nevertheless, for both U values, the total magnetic moments of CP are in excellent agreement with the experimental data ($\sim 4.95\mu_B$). On going from U=0 to 6.0 eV, the magnetic moment of CP is found to remain mainly localized on Mn ($3.84\mu_B$ to $4.54\mu_B$), with small contributions from Ce ($-0.14\mu_B$ to $-0.10\mu_B$) and Ni ($0.29\mu_B$ to $0.14\mu_B$).

Our LDA+U calculations for the CP of $CeMnNi_4$ indicate that the local magnetic moments obtained for all Ce (and Mn) atoms in the cubic supercell are identically the same. This implies neither Ce nor Mn tends to be in a mixed-valent state. For the former, the f states appear to be nearly empty in both spin channels. Consequently, as mentioned earlier

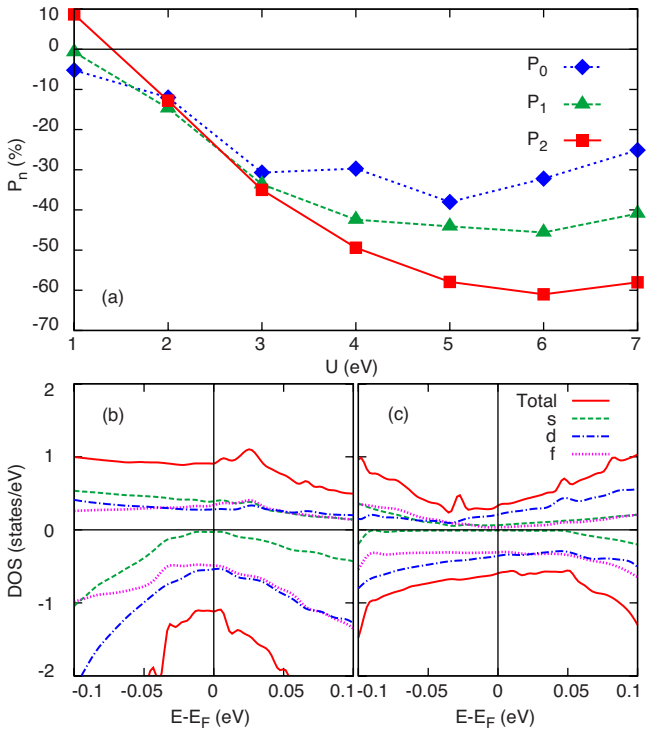

FIG. 4. (Color online) (a) Dependence of P_n to U on Mn $3d$. Total and partial density of states of cubic $CeMnNi_4$ computed for (b) $U=0$ ($J=0$) and (c) $U=6.0$ eV ($J=0.8$ eV). The s contributions are scaled up by 10.

PDOS of Ce f bands lies approximately 1 eV above ε_F (see Figs. 2 and 3). The variation in U on Mn, as might be expected, turns out to have hardly any effect on PDOS of Ce f states. Considering an atomic sphere with radius of 2.32 Å for Ce, the Ce charge is estimated to be around $1.3e$ which is in close agreement with the corresponding result, $1.2e$, obtained from the previous full potential linearized augmented plane waves calculations.[6] For Mn, it has been experimentally observed that it is in its highest spin state, Mn^{2+}.[4,16] Considering the total magnetization of $4.95\mu_B$ for CP of $CeMnNi_4$, this implies that all the five d states of Mn in spin-up (spin-down) channel should be almost completely occupied (unoccupied). Increasing U on Mn, one can clearly notice that exchange splitting between Mn $3d$ states in opposite spin channels becomes so significantly large that all the spin-up $3d$ states tend to be completely occupied while the corresponding spin-down $3d$ states are substantially shifted above ε_F and, hence, nearly empty (see Fig. 2). Therefore, in accordance with the experimental findings, we expect Mn in $CeMnNi_4$ to be in a divalent charge state, that is, Mn^{2+}.

Having clarified why GGA fails to reproduce the experimental CP as the ground-state structure of $CeMnNi_4$, we further show below that by introducing the U correction on the Mn $3d$ states, the reason for the failure of conventional DFT methods in reproducing the experimental P value of $CeMnNi_4$ can also be understood. Similar to what was previously reported in Ref. 8, the PW91 calculations result in $P_0=-9.5\%$, $P_1=-2.2\%$, and $P_2=9.3\%$ which are much lower than the experimental value of 66%.[17]

By increasing U on Mn $3d$, we have found that the absolute value of P_n in both ballistic and diffusive regimes as well as the static one increases sharply. The dependence of P_n to U^{3d}_{Mn} has been demonstrated in Fig. 4(a). The trend is $|P_2|>|P_1|>|P_0|$ (except for $U=2.0$ eV). Interestingly, P_2 after a rather sharp decline tends to converge to the experimental P value. For $U=6.0$ eV, $|P_2|$ value turns out to be $\sim 64\%$, which is in excellent agreement with experiment.[4] Such a good agreement reiterates our conclusion that U on Mn $3d$ states should be 6.0 eV. This is the optimum value by which both the structural phase stability and spin-dependent transport of $CeMnNi_4$ can be well described.

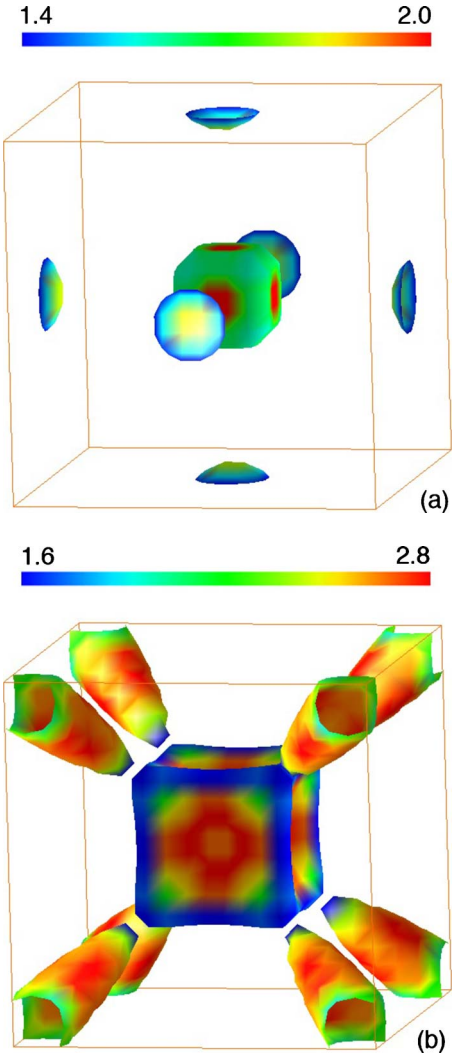

FIG. 5. (Color online) Fermi surfaces of $CeMnNi_4$ in (a) spin-up and (b) spin-down channels. The Fermi velocity values are in 10^7 cm/s.

To understand why the P_n values tend to increase by increasing U on Mn $3d$ states, in Figs. 4(b) and 4(c), we have shown PDOS as well as the total density of states for $CeMnNi_4$ in the vicinity of ε_F at $U=0$ and 6.0 eV, respectively. In the GGA limit, one can clearly notice that $N_\uparrow$ is slightly smaller than $N_\downarrow$, thus, P_0 turns out to be negative and rather small. However, since the contribution of light s electrons to $N_\uparrow$ is much larger than that of heavy d and f electrons, $v_{F\uparrow}=2.2\times 10^7$ cm/s becomes larger than $v_{F\downarrow}=1.5$

$\times 10^7$ cm/s, leading to a sign difference between P_0 and P_2, as explained in Ref. 8. On the other hand at $U=6.0$ eV, $N_\uparrow$ and $N_\downarrow$ undergo significant changes so that $N_\uparrow \ll N_\downarrow$. The former appears to be predominately Ni $3d$ like, whereas the latter is dominated equally by Ni $3d$ and Ce $4f$ electrons. Evidently, there is no contribution from Mn $3d$ states due to the U localization. Additionally, the s contributions in both spin channels become nearly zero. Accordingly, with U switched on, $v_{F\downarrow}=2.17\times 10^7$ cm/s turns out to be larger than $v_{F\uparrow}=1.58\times 10^7$ cm/s. The facts that both $N_\uparrow$ and $v_{F\uparrow}$ are smaller than the corresponding spin-down quantities thus justify why P_n are all negative and, more importantly, why $|P_2|>|P_1|>|P_0|$.

The corresponding Fermi surfaces of cubic $CeMnNi_4$ at $U=6.0$ eV have been shown for both spin states in Fig. 5. The Fermi surfaces are mainly formed by three bands, one for spin-up channel and two for the spin-down one, similar to that obtained at $U=0$.[6] This indicates that $CeMnNi_4$ is not expected to exhibit very good metallic properties. The calculated $v_{F\uparrow}$ and $v_{F\downarrow}$ further denotes that the carrier mobility in this compound is relatively lower than that of conventional metallic systems. While the variation in U on Mn $3d$ appears to have little effect on the Fermi surfaces in spin-down channel (compare Fig. 5 with Fig. 6 of Ref. 6), the Fermi surface in spin-up channel gets strongly squeezed, resulting in the high degree of transport spin polarization, as experimentally observed by the PCAR experiments.[4]

At this point it is worth mentioning as to why Mn may have such a large value of $U=6.0$ eV in a pure intermetallic compound. We believe that, the reason is due to the anomalously large Mn-Ni and Mn-Ce bond distances in CP of $CeMnNi_4$. As mentioned earlier, the respective distances are 2.89 and 3.02 Å. Thus, the Mn ions appear to be trapped in a cage much larger than is needed for normal metallic bondings. As a result, they are expected to have lower tendency for hybridization with their neighbors. This is the reason why Mazin had previously proposed that Mn is more likely a "rattling" ion, loosely bounded to its neighbors;[6] a prediction which was later confirmed experimentally.[16] Accordingly, it seems to be justifiable why our calculations predict a relatively large U for Mn. The confirmation of our prediction, however, requires further experimental studies, such as the X-ray photoemission spectroscopy (XPS). It is to be noted that the XPS valence-band spectra for $CeMn_{0.8}Ni_{4.2}$ has been already reported by Klimczak *et al.*[18] However, since this compound crystallizes in a hexagonal phase with supposedly different Mn-Ni and Mn-Ce distances, we think it is necessary to perform similar study on the cubic $CeMnNi_4$ so that one can have a correct comparison between the value of U^{3d}_{Mn} obtained from our calculations with the corresponding experimental data.

In summary, we have shown that the LDA+U approach can be utilized to successfully describe the structural stability, magnetism, and spin-dependent transport in $CeMnNi_4$. The overdelocalization of Mn $3d$ states turns out to be the reason for the failure of conventional LDA and GGA approaches in reproducing the experimentally observed stabilization of the compound in cubic phase and its high degree of current spin polarization. The variation in U on Ce $4f$ and Ni $3d$ bands hardly plays any role in describing the ground-state properties of $CeMnNi_4$. Our theoretical findings suggest further XPS-based experimental studies to determine the extent to which the Mn $3d$ states are localized in this intermetallic compound.

We thank the staff of the Center of Computational Materials Science at the Institute for Materials Research for the use of the Hitachi SR11000-K2 supercomputing facilities. M.S.B. gratefully acknowledges support from the Japan Society for Promotion of Science. G.P.D. acknowledges support from BRNS under CRP. The authors thank P. Raychaudhuri for helpful discussions.

*Present address: Advanced Science Institute, RIKEN, Hirosawa 2–1, Wako, Saitama 351-0198 Japan. bahramy@riken.jp

[1] W. E. Pickett, Rev. Mod. Phys. **61**, 433 (1989).
[2] A. Svane and O. Gunnarsson, Phys. Rev. Lett. **65**, 1148 (1990).
[3] V. I. Anisimov, J. Zaanen, and O. K. Andersen, Phys. Rev. B **44**, 943 (1991).
[4] S. Singh, G. Sheet, P. Raychaudhuri, and S. K. Dhar, Appl. Phys. Lett. **88**, 022506 (2006).
[5] E. N. Voloshina, Y. S. Dedkov, M. Richter, and P. Zahn, Phys. Rev. B **73**, 144412 (2006).
[6] I. I. Mazin, Phys. Rev. B **73**, 012415 (2006).
[7] P. Murugan, A. K. Singh, G. P. Das, and Y. Kawazoe, Appl. Phys. Lett. **89**, 222502 (2006).
[8] M. S. Bahramy, P. Murugan, G. P. Das, and Y. Kawazoe, Phys. Rev. B **75**, 054404 (2007).
[9] L. Nordström, M. S. S. Brooks, and B. Johansson, Phys. Rev. B **46**, 3458 (1992).
[10] J. P. Perdew, in *Electronic Structure of Solids 91*, edited by P. Ziesche and H. Eschrig (Akademie Verlag, Berlin, 1991), p. 11; J. P. Perdew and Y. Wang, Phys. Rev. B **45**, 13244 (1992).
[11] J. P. Perdew, J. A. Chevary, S. H. Vosko, K. A. Jackson, M. R. Pederson, D. J. Singh, and C. Fiolhais, Phys. Rev. B **46**, 6671 (1992); Phys. Rev. B **48**, 4978(E) (1993).
[12] P. E. Blöchl, Phys. Rev. B **50**, 17953 (1994).
[13] G. Kresse and J. Furthmüller, Phys. Rev. B **54**, 11169 (1996); Comput. Mater. Sci. **6**, 15 (1996); G. Kresse and D. Joubert, Phys. Rev. B **59**, 1758 (1999).
[14] O. K. Andersen, Phys. Rev. B **12**, 3060 (1975).
[15] I. I. Mazin, Phys. Rev. Lett. **83**, 1427 (1999).
[16] I. Dhiman, A. Das, S. K. Dhar, P. Raychaudhuri, S. Singh, and P. Manfrinetti, Solid State Commun. **141**, 160 (2007).
[17] The P_n values as well as Fig. 4(b) correspond to the current $(20\times 20\times 20)$ k-converged results and hence somewhat differ from our earlier data in Ref. 8 with $(8\times 8\times 8)$ k mesh.
[18] M. Klimczak, E. Talik, J. Kusz, A. Kowalczyk, and T. Toliński, Cryst. Res. Technol. **42**, 1348 (2007).